The nephelauxetic effect on the electron binding energy in the $4f^q$ ground state of lanthanides in compounds

Dorenbos, Pieter

DOI
10.1016/j.jlumin.2019.116536

Publication date
2019

Document Version
Accepted author manuscript

Published in
Journal of Luminescence

Citation (APA)
Dorenbos, P. (2019). The nephelauxetic effect on the electron binding energy in the $4f^q$ ground state of lanthanides in compounds. *Journal of Luminescence*, *214*, Article 116536. https://doi.org/10.1016/j.jlumin.2019.116536

The nephelauxetic effect on the electron binding energy in the $4f^q$ ground state of lanthanides in compounds.

Pieter Dorenbos

Delft University of Technology,

Faculty of Applied Sciences,

Department of Radiation Science and Technology,

Section Luminescence Materials,

Mekelweg 15, 2629 JB Delft, Netherlands

email:p.dorenbos@tudelft.nl

tel: +31 15 2781336

(Dated: July 10, 2019)

Abstract

In the construction of a vacuum referred binding energy (VRBE) diagram with the lanthanide $4f^q$ ground states, always a compound independent variation with the number $q = 1$ to 14 is assumed. Experimental data from thermo-luminescence, intervalence charge transfer bands, and thermo-bleaching studies provide first indications that a minor compound dependence does exist. To explain its origin we will first apply the Jørgensen spin pairing theory to reproduce the VRBE in the ground states of the free di- and trivalent lanthanide ions which is equivalent to the 3^{rd} and 4^{th} ionization potentials of the lanthanide atoms. By combining experimental data and calculated trends therein, the relevant Racah E^1, Racah E^3, and spin orbit coupling ζ_{ff} parameters for all di-, tri-, and tetravalent free ion lanthanides are derived. Using that as input for the spin pairing theory, the characteristic zigzag shapes in VRBE as function of q, as derived from ionization potentials, are nicely reproduced. Because of the nephelauxetic effect the parameter values are lowered when lanthanides are in compounds. How that reduction affects the VRBE curves will be treated in this work.

I. INTRODUCTION

The energy needed for an electronic transition from a lanthanide impurity state to a host valence band (VB) or conduction band (CB) state or vice versa provides information on the location of that impurity state within the band gap of the compound [1]. Hole release from a lanthanide to the VB or electron release to the CB can be probed by thermoluminescence (TL) or by photoconductivity (PC) techniques. Electron transfer from the VB-top to a lanthanide or from a lanthanide to the CB-bottom are manifest as so-called charge transfer (CT) or intervalence charge transfer (IVCT) bands in absorption or luminescence excitation spectra.

From gathering information on CT-energies always the same characteristic variation in lanthanide ground state level location with the number of electrons in the 4f-orbital appears. This has led to empirical models to construct so-called host referred binding energy (HRBE) schemes with all divalent and all trivalent lanthanide $4f^n$ ground state locations with respect to the host bands. In 2012 the chemical shift model was developed [3] to convert such HRBE scheme into a vacuum referred binding energy scheme (VRBE) where all energies are referred to the vacuum level, i.e., the energy of an electron with zero kinetic energy in the vacuum.

Figure 1 shows the VRBE scheme for YPO_4. The zigzag curve $Ln^{2+/3+}$ connects the $4f^q$ ground state locations of divalent lanthanides. The energy difference with the CB-bottom is then the energy needed for electron ionization from Ln^{2+} that can be probed with TL or PC, see for example arrow 1 for Nd^{2+}. The same curve represents the electron acceptor levels of the trivalent lanthanides. The energy difference with the CB-bottom is then the trivalent lanthanide electron trapping depth (see arrow 2 for Tm^{3+}). The energy difference with the VB-top is equivalent to the CT-band energy observed in excitation spectra of trivalent lanthanide luminescence (see arrow 3 for Yb^{3+}). The zigzag curve $Ln^{3+/4+}$ connects the ground state locations of the trivalent lanthanides but can equally well be treated as the curve that connects the CB electron acceptor states of the tetravalent lanthanides. The energy difference with the VB-top is the energy needed for hole ionization from Ln^{4+} that can be probed with TL (see arrow 4 for Pr^{4+} and arrow 5 for Tb^{4+}).

During the past two decades, the shapes of the two zigzag curves were revised several times to eventually evolve in the latest ones from [1] that was used for Fig. 1. Since there

were no experimental indications for a compound dependence, the same zigzag shapes are used for all type of compounds. However recently, indications that the trivalent lanthanide zigzag curve must be compound dependent were found [2]. With TL, the energy for hole release from Pr^{4+} was compared with that from Tb^{4+} for various compounds. Without such dependence, one expects that the energy difference will be constant. However that difference changes by about 0.1 to 0.15 eV when going from a phosphate, to silicate, to aluminate compound.

By comparing TL-data on electron release from divalent lanthanides with 60 years old thermo-bleaching data, one can also derive evidence for a compound dependence in the $Ln^{2+/3+}$ binding energy curve. Figure 2 shows the thermoluminescence glow curves due to the release of an electron trapped on divalent Er, Nd, Ho, Dy, and Tm in $GdAlO_3$ which then recombines with a hole trapped on Ce^{3+} to generate Ce^{3+} 5d-4f luminescence [4]. Glow peak analysis shows that a 0.01 eV increase in trapping depth already leads to ≈3K shift of the glow peak maximum T_m which demonstrates a very high sensitivity of T_m to the precise shape of the $Ln^{2+/3+}$ VRBE curve. The maximum temperature of the glow peak for Nd from the left hand side of the VRBE curve falls in between that of Er and Ho from the right hand side. The same applies to other oxides like YPO_4 and $LaPO_4$ [1]. This is consistent with the $Ln^{2+/3+}$ VRBE curve in Fig. 1 as illustrated by the horizontal dashed line.

Fig. 3 shows results on the thermobleaching of divalent lanthanide absorption bands in CaF_2:Sm^{2+};Ln^{3+} (Ln = Er, Ho, Nd, Dy) reproduced from the 1969 work of Arkangelskaya *et al.* [5]. Prior to the bleaching, electrons are transferred from Sm^{2+} to the trivalent lanthanide by photon excitation. It creates absorption bands of divalent Er, Ho, Nd, or Dy. Next, the crystal is heated while monitoring the absorption intensity. The moment electrons can escape from the divalent lanthanide ground state, a bleaching of the absorption band is observed and one can define the temperature T_{50} where absorption has bleached by 50%. T_{50} for Er, Ho, and Dy in CaF_2 appears at about 290 K higher temperature then the T_m for the same lanthanides in $GdAlO_3$. This means that the electron trap for all three lanthanides in CaF_2 is a fixed amount deeper as compared to $GdAlO_3$. Such fixed amount is consistent with a compound independent shape of the VRBE curve. Note that the T_{50} for Nd falls in between that of Ho and Dy in CaF_2 whereas the glow peak of Nd in $GdAlO_3$ falls in between that of Er and Ho. This is not consistent with a compound independent shape. It suggests that in CaF_2 the Dy, Ho, and Er divalent ground states are raised by about 0.15 eV

with respect to that of Nd^{2+}. Considering above findings, we need to introduce a compound dependence in the shape of the zigzag curves that should be of the order of few 0.1 eV. In this work we will demonstrate that by combining the nephelauxetic effect on the $^{2s+1}L_J$ $4f^q$ level energies with the spin pairing theory of Jørgensen [6, 7] this can all be explained.

The typical zigzag shapes in the binding energies for the 2+ and 3+ lanthanide ions also appear in the 3^{rd} and 4^{th} ionization potentials of the lanthanides, and it was long time ago qualitatively explained with the spin pairing theory of Jørgensen [6, 7]. In that theory the interelectron Coulomb repulsion between the 4f electrons in the free lanthanides is parameterized by the Slater-Condon F^k $(k = 0, 2, 4, 6)$ parameters and the spin-orbit coupling parameter $\zeta_{\rm ff}$. In this work we will apply the spin pairing theory to quantitatively reproduce the ionization potentials where we will follow a somewhat different route than in previous attempts.

The parameters of interelectron repulsion that determine the binding energy in the ground state multiplets equally well determine the binding in the excited state $^{2S+1}L_J$ multiplets of the lanthanides. Figure 4 shows the energies of the 13 $^{2S+1}L_J$ $4f^2$ energy levels for Pr^{3+} as free ion from [8], in LaF_3 from [9, 10], and in La_2O_3 from [11] relative to that of the $^3H_4$ ground state. In compounds, the excited state energies are lowered with respect to the ground state due to a decrease in interelectron repulsion which is attributed to the nephelauxetic effect. Nephelauxetic is Greece for cloud expansion. It has been studied in great detail in many papers to explain the excited state energies of the lanthanides in compounds, but its effect on the VRBE of the lanthanide ground states has never been studied. One expects that changes in the interelectron repulsion will affect the ground state energies with respect to the vacuum level which, unless the change is the same for each lanthanide, implies that the two zigzag curves in Fig. 1 should be compound dependent. The results in Fig. 2 and Fig. 3 suggest that when going from fluorides to oxides, the ground state energy of divalent Dy, Ho, and Er on the right hand branch lower by about 0.15 eV with respect to that of divalent Nd on the left hand branch. Similar applies for the ground state energy of Tb^{3+} from the right hand branch with respect to that for Pr^{3+} from the left hand branch.

In this work we will first establish the Slater F^k and $\zeta_{\rm ff}$ parameters for the di, tri, and tetravalent free lanthanides by combining experimental data with calculated trends on how they change with the number of 4f electrons. Next the contribution of the interelectron repulsion to the binding energy in the ground states is determined. By using the data on

the 3^{rd} and 4^{th} ionization potentials we will derive smoothly varying functions with q for the binding of a 4f electron to the nucleus with the [Xe] core configuration. Finally the effect of the chemical shift, the lanthanide contraction and the nephelauxetic effect on the VRBE in the lanthanide ground state multiplets when in a chemical environment will be treated. We will show that the nephelauxetic effect can lower the VRBE for the right hand branch($q > 7$) of the zigzag curve by about 0.5 eV depending on the type of chemical environment or inorganic compound. This nephelauxetic lowering explains the observation in Fig. 2 and 3. The amount of nephelauxetic variation within the oxide compounds remains within ± 0.1 eV and this is consistent the hitherto used approximation that the shape of the VRBE curves is invariant within ± 0.1 eV.

II. THEORY

The theory on the energy differences between the $4f^q$ levels within a lanthanide ion is well-established. Always the $4f^q$ ground state is then the level of reference, which is placed conveniently at energy zero as in Fig. 4. In this work we are interested in the energy differences between the ground states of two different lanthanides, and then we need a common reference of energy like the vacuum level in Fig. 1. Knowledge on these energy differences provides us with the shapes of the zigzag curves in binding energies. The energy differences within the lanthanides must be strongly tied with the energy differences between the lanthanides. Once this is established theoretically, knowledge on energy differences within a lanthanide can be utilized to determine energy differences between lanthanides.

For a free lanthanide ion, each electron in the $4f^q$ orbital has the same interaction with the nucleus and with the electrons of its closed shell [Xe] configuration [12]. This means that the energy differences between the $4f^q$ levels within a lanthanide are, ignoring spin-orbit interaction, only determined by the repulsive Coulomb interaction between the electrons within the $4f^q$ orbitals. The levels are like in Fig. 4 usually labelled with the $^{2s+1}L_J$ term symbols where L, S, and J are the quantum numbers for angular momentum, spin momentum, and total momentum of all q electrons together. The Coulomb repulsion between $4f^q$ electrons is commonly expressed by the Slater integrals, and the value of those integrals for each $4f^n$ LS-term can be expressed with the four Slater-Condon parameters F^0, F^2, F^4, and F^6. These are all positive numbers that we will express in eV, and are determined exclusively by

the radial functions $R_{4f}(r)$. Calculations on the free lanthanide ions by Ma *et al.* [13] reveal that $F^4 \approx 0.625F^2$ and $F^6 \approx 0.45F^2$. The proportionality constants are almost independent on atomic number and valence (2+, 3+, 4+). An LS-term will be further split by the spin orbit coupling leading to $2J + 1$ different $^{2s+1}L_J$ levels.

Optical spectroscopy of a lanthanide as a free ion or as a dopant in a compound provides detailed information on the excited state level energies with respect to the ground state. To understand and reproduce the rich level structure of the lanthanides, interactions between 4f electrons and with the crystal field were parameterized in terms of the F^k parameters, the spin orbit coupling parameter ζ_{ff}, the two body configuration interaction or Trees parameters α, β, and γ, the B_{qk} crystal field parameters, and additional parameters of less importance [14]. The parameter values can then be obtained by fitting the theoretical expressions to the experimentally observed $^{2s+1}L_J$ level energies. The crystal field parameters depend on the site symmetry and bond lengths. The F^k parameters appear not to correlate with the crystal field parameters but to the nephelauxetic effect [15]. Tanner and Yeung [14] reviewed the experimental parameters for Pr^{3+} as free ion and for Pr^{3+} in compounds paying special attention to the nephelauxetic effect and how that relates to the reduction of the F^k parameters. Their conclusion based on a careful analysis and following ideas of Morrison [16, 17] and Newman [18] is that the parameter reduction and nephelauxetic effect is tied to the polarizability of the surrounding ligands. Since the F^k and the spin orbit coupling parameter ζ_{ff} are the dominant parameters that determine level energies we will only consider the effect of those parameters on the VRBE in the ground state $4f^q$ level. The two body interaction parameters that emanate from second order perturbation theory [19], the crystal field parameters and others will not be further considered.

Instead of the F^k parameters often the E^0, E^1, E^2, and E^3 Racah parameters are used to parameterize the inter-electron repulsion. They are positive numbers (energies) and linear combinations of the F^k parameters as in the following expressions.

$$E^0 = F^0 - \frac{2}{45}F^2 - \frac{1}{33}F^4 - \frac{50}{1287}F^6 \approx F^0 - 8.08 \times 10^{-2}F^2 \tag{1}$$

$$E^1 = \frac{14}{405}F^2 + \frac{7}{297}F^4 + \frac{350}{11583}F^6 \approx 6.29 \times 10^{-2}F^2 \tag{2}$$

$$E^2 = \frac{1}{2025}F^2 - \frac{1}{3267}F^4 + \frac{175}{1656369}F^6 \approx 3.50 \times 10^{-4}F^2 \tag{3}$$

$$E^3 = \frac{1}{135}F^2 + \frac{2}{1089}F^4 - \frac{175}{42471}F^6 \approx 6.70 \times 10^{-3}F^2 \quad (4)$$

Using the more or less constant ratios between the F^k parameters as established in the calculations by Ma *et al.*, [13] the E^1 , E^2, and E^3 Racah parameters can be approximately expressed in terms of F^2. Note that E^3 is about ten times smaller than E^1. The energy differences between the $^{2s+1}L_J$ levels within the lanthanides are independent on F^0. Therefore, spectroscopy cannot supply an experimental value for the F^0 parameter and, as consequence, the E^0 Racah parameter.

The same parameters that control the separation between the $4f^q$ levels within a lanthanide ion also control the binding energy in the ground state with respect to the vacuum level. We will use the expression from [20] for the total energy $E(4f^q, Q, \text{vacuum})$ (in short $E(4f^q)$ or $E(4f^q, Q)$) of all q electrons in a $^{2s+1}L_J$ $4f^q$-state

$$E(4f^q) = -qW - \frac{q(q-1)}{2}(E^* - E^0) + \frac{9}{13}[\frac{q(q-1)}{2} + n(S)]E^1 + m(L)E^3 + p(S,L,J)\zeta_{\text{ff}} \quad (5)$$

$$E(4f^q, Q) = c(q, Q) + s(q, Q) \quad (6)$$

Here $-W$ represents the binding energy of one 4f electron to the nucleus together with the [Xe] electron core. E^* is a parameter to account for the stabilization of 4f electrons due to the increase of the effective nuclear charge from one lanthanide to the next. The first two terms together are assumed to be a smooth, but yet unknown, function with q. It will be denoted as function $c(q, Q)$. The last three terms together define $s(q, Q)$ and contain the e-e repulsion and spin orbit interaction in a $^{2s+1}L_J$ state of the $4f^q$ configuration. We added the variable Q to the functions E, c and s in Eq. (6) to denote the valence ($Q = 2+$, $3+$, or $4+$) of the lanthanide. $n(S)$, $m(L)$, and $p(S, L, J)$ are coefficients that emanate from Jørgensons spin pairing theory. Column 6, 8, and 9 of Table I lists the values for those coefficients for the $^{2s+1}L_J$ ground state term symbols in column 5. Columns 7 shows the coefficients for the E^1 contribution to Eq. (5).

The energy $E_{4f}(q, Q, A)$ needed to remove an electron from the ground state of the $4f^q$ configuration of an Ln^Q in a chemical environment A, and to bring it to the vacuum level is defined as the vacuum referred binding energy of that electron. It is equivalent to

TABLE I: The coefficients for the energy terms of the interelectron repulsion and spin-orbit interaction for lanthanides with the $4f^q$ configuration in the refined spin pairing energy theory.

q	Ln^{2+}	Ln^{3+}	Ln^{4+}	g.s.	$n(S)$	$\frac{9}{13}[\frac{q(q-1)}{2}+n(S)]$	$m(L)$	$p(S,L,J)$
0	–	La	Ce	$^1S_0$	0	0	0	0
1	La	Ce	Pr	$^2F_{5/2}$	0	0	0	-2
2	Ce	Pr	Nd	$^3H_4$	-1	0	-9	-3
3	Pr	Nd	Pm	$^4I_{9/2}$	-3	0	-21	-7/2
4	Nd	Pm	Sm	$^5I_4$	-6	0	-21	-7/2
5	Pm	Sm	Eu	$^6H_{5/2}$	-10	0	-9	-3
6	Sm	Eu	Gd	$^7F_0$	-15	0	0	-2
7	Eu	Gd	Tb	$^8S_{7/2}$	-21	0	0	0
8	Gd	Tb	Dy	$^7F_6$	-15	9	0	-3/2
9	Tb	Dy	Ho	$^6H_{15/2}$	-10	18	-9	-5/2
10	Dy	Ho	Er	$^5I_8$	-6	27	-21	-3
11	Ho	Er	Tm	$^4I_{15/2}$	-3	36	-21	-3
12	Er	Tm	Yb	$^3H_4$	-1	45	-9	-5/2
13	Tm	Yb	Lu	$^2F_{7/2}$	0	54	0	-3/2
14	Yb	Lu	–	$^1S_0$	0	63	0	0

$$E_{4f}(q,Q,A) = E(4f^q,Q,A) - E(4f^{q-1},Q+1,A) \tag{7}$$

In early treatments on this energy difference for the free lanthanides, the Racah and $\zeta_{\rm ff}$ parameters were assumed independent on q and Q [7, 21]. Van der Sluis and Nugent [22] realized that one should take a q dependence into account. However, in Eq. (7) there is also a Q and A dependence which, different from previous work, will be taking into account here. Apart from La^{2+} and Gd^{2+}, $E_{4f}(q,2+,\text{vacuum})$ and $E_{4f}(q,3+,\text{vacuum})$ are equivalent to the negative of the 3^{rd} and 4^{th} ionization potentials of the lanthanide atoms. For La^{2+} and Gd^{2+} the lowest $4f^{q-1}$ 5d level is the ground state and the ionization energy must then be corrected for the $4f^q$ to $4f^{q-1}5d$ energy difference. The $E_{4f}(q,Q,\text{vacuum})$ values as also compiled in [3] are reproduced in Table II.

Inserting Eq. (5) into Eq. (7) for the free lanthanides, the difference $C(q,Q) \equiv$

TABLE II: Atomic number Z, $E_{4f}(q, Q, \text{vacuum})$ (in eV) and the Shannon ionic radii $R(q, Q)$ in pm of the divalent and trivalent lanthanide ions. We used the tabulated radii for lanthanides in 8-fold coordination from [23].

Z	Ln	$E_{4f}(q, 2+)$	$E_{4f}(q, 3+)$	$R(q, 2+)$	$R(q, 3+)$
57	La	-18.286	–	148.7	130.0
58	Ce	-20.198	-36.758	147.0	128.3
59	Pr	-21.624	-38.98	145.3	126.6
60	Nd	-22.102	-40.6	143.7	125.0
61	Pm	-22.369	-41.2	142.2	123.4
62	Sm	-23.601	-41.6	140.7	121.9
63	Eu	-24.92	-42.97	139.3	120.5
64	Gd	-20.335	-44.5	137.9	119.2
65	Tb	-21.91	-39.37	136.6	117.9
66	Dy	-22.89	-41.2	135.4	116.7
67	Ho	-22.84	-42.4	134.3	115.6
68	Er	-22.74	-42.5	133.2	114.5
69	Tm	-23.68	-42.4	132.2	113.5
70	Yb	-25.03	-43.56	131.3	112.5
71	Lu	–	-45.25	–	111.7

$c(q, Q,) - c(q-1, Q+1)$ between two expected smooth functions is again expected to be a smooth function. The difference $S(q, Q) \equiv s(q, Q) - s(q-1, Q+1)$ can be computed by using experimental and or best estimated values for the Racah parameters and ζ_{ff} and the coefficients from Table I. By subtracting the $S(q, Q)$ parts from the listed $E_{4f}(q, Q, \text{vacuum})$ values in Table II, we will first derive the smooth functions $C(q, Q)$. For divalent and trivalent free lanthanides they will indeed turn out to be smoothly varying with q. Next we will use experimental or estimated values for the Racah parameters in compounds like LaF_3, $LaCl_3$, YPO_4, and La_2O_3 to explore how that affects the shape of the zigzag curves in VRBE diagrams.

III. RESULTS ON THE LANTHANIDES IN VACUUM

To employ Eq. (7) to reproduce the binding energy curve for the divalent and trivalent lanthanides we need the Slater parameters (or Racah parameters) and $\zeta_{\rm ff}$, for the divalent, trivalent and tetravalent lanthanides. For that we will make use of the calculated parameters by Ma *et al.* [13]. To very good approximation the F^k and $\zeta_{\rm ff}^{1/4}$ increase linearly with the atomic number Z, or equivalently with the number of electrons in the 4f-orbital. Therefore, instead of compiling the values for each lanthanide individually we can work with the linear relationships that are reproduced in Table III.

TABLE III: The linear relationships with atomic number Z for the calculated Slater parameters and calculated $\zeta_{\rm ff}^{1/4}$ for divalent, trivalent, and tetravalent free lanthanide ions. Data are from [13] and in eV.

	F^2	F^4	F^6	$\zeta_{\rm ff}^{1/4}$
Ln^{2+}	$-16.17+0.456Z$	$-10.24+0.286Z$	$-7.400+0.206Z$	$2.42510^{-5}(Z-32.73)$
Ln^{3+}	$-11.63+0.403Z$	$-7.233+0.251Z$	$-5.187+0.181Z$	$2.26610^{-5}(Z-29.73)$
Ln^{4+}	$-8.981+0.377Z$	$-5.448+0.234Z$	$-3.866+0.168Z$	$2.18310^{-5}(Z-27.64)$

Figures 5, 6, 7 show the experimentally known values for the Slater parameters for the free di-, tri-, and tetravalent lanthanides. That of the divalent lanthanides Ce, Eu, and Er are from [24–26], the trivalent lanthanides Pr, Nd, Er, Tm from [14, 27–29], and the tetravalent Nd, and Yb from [27, 30]. The dashed lines are the calculated linear relationships from Table III corrected with a constant value chosen such that the lines run through the experimental data points. The values of the constants are written within brackets along the dashed lines. Although only a limited set of experimental data is available, it appears that the calculated increase of F^k with atomic number is very well confirmed by the data. The needed constant energy shift appears not to depend much on the lanthanide charge. Note that the value for all three F^k parameters increase with the charge Q of the lanthanide but that the rate of change with Z decreases with Q.

Figure 8 shows experimental data on the spin-orbit coupling parameters $\zeta_{\rm ff}$ for the free lanthanides. Ce^{2+} is from [24], Pr^{3+}, Nd^{3+}, and Nd^{4+} from [27], Eu^{2+} from [25], Er^{2+} from [26], Er^{3+} from [28], Tm^{3+} from [29], and Yb^{4+} from [30]. The solid curves connect the calculated results from [13] that are listed in Table III. The curves are shifted with a small

amount to adjust them better to the experimental data.

In the following we regard the dashed lines and curves in Figure 5, 6, 7, and 8 as our best representatives for the free ion F^k and $\zeta_{\rm ff}$ values. It provides with Eq. (2) and Eq. (4) all the parameters needed to calculate with Eq. (5), Eq. (7) and Table I the spin pairing contributions $S(q, Q)$ to the binding energies $E_{4f}(q, Q, \text{vacuum})$.

IV. RESULTS ON THE LANTHANIDES IN A CHEMICAL ENVIRONMENT

When lanthanides are placed in a chemical environment one has to deal with the interactions between the 4f electrons with that chemical environment. The main interaction is the Coulomb repulsion with the surrounding negative charge from the anions. This repulsion generates a chemical shift in binding energy towards less negative values. The nature, the size, and compound variation therein can be treated with the chemical shift model introduced in 2012 [3]. Effectively a 2+ lanthanide is surrounded by 2- charge at a screening distance R_{2+}. The screening distance appears slightly larger than the Shannon ionic radius $R(q, 2+)$ of the lanthanide in Table II. Similarly a 3+ lanthanide is screened by 3- charge at screening distance R_{3+} that is somewhat smaller than R_{2+}. As a consequence the chemical shift for Ln^{3+} will be slightly more than a factor 3/2 larger than for Ln^{2+}. The $U(6, A)$-value for Eu defined in Eq. (8) is then reduced from the free Eu ion value of 18.05 eV to values that appear to range between 7.6 eV and 6.1 eV for Eu in inorganic compounds [31]. It is for example 7.09 eV for YPO_4 in Fig. 1 as indicated by the dashed arrow.

$$U(6, A) = E_{4f}(7, 2+, A) - E_{4f}(6, 3+, A). \tag{8}$$

The changing $U(6, A)$ value is directly linked to a compound dependent screening distance. For compounds with strongly bonded anion ligands as in fluorides, the ligands cannot optimally screen the lanthanide charge which, within the chemical shift model, translates to a larger screening distance, relatively small chemical shift and large $U(6, A)$. When ligands are more weakly bonded as in chlorides, bromides, iodides screening is more efficient leading to smaller screening distances, larger chemical shift, and smaller $U(6, A)$. For the pure lanthanide metals screening is most efficient and chemical shift is maximal and $U(6, A)$ becomes minimal. The empirical relation between $U(6, A)$ and the chemical shift $E(7, 2+, A)$ or $E(Eu, 2+, A)$ for divalent Eu is given by Eq. (9) and Eq. (10) from [3].

$$E(Eu, 2+, A) = \frac{18.05 - U(6, A)}{0.777 - 0.0353U(6, A)} \tag{9}$$

$$E(Eu, 3 + A) = E(Eu, 2+, A) + 18.05 - U(6, A) \tag{10}$$

Above equations all apply to Eu. Because of the lanthanide contraction, the screening radius R_Q will decrease and the size of the chemical shift will increase from the beginning towards the end of the lanthanide series. Assuming that the screening radius changes proportional with the difference in ionic radius of Eu this results, next to an upward shifting, also into a tilting of the free ion binding energy curve. One may write

$$E_{4f}(q, Q, A) = E_{4f}(q, Q, \text{vacuum}) + \text{E(Eu, Q, A)} + \alpha(\text{Q})(\text{R(Eu, Q)} - \text{R(q, Q)}) \tag{11}$$

where a tilt parameter of $\alpha(3+) = 0.11$ eV/pm and $\alpha(2+) = 0.075$ eV/pm provided best agreement with experimental derived binding energy curves in [3].

In the construction of the VRBE diagrams for the lanthanides in compounds, the only compound dependent parameter is the $U(6, A)$ value. A compound dependent tilt was always ignored, and possible effects of compound dependence of Racah values were also never addressed. Figure 9 shows the F^k parameters for the trivalent lanthanides in $LaCl_3$ as reported by Yeung and Tanner [32]. The same figure shows the linearized parameters for the free ions reproduced from Figure 6. The parameters for $LaCl_3$ are about 5% smaller than that for the free ions which must be attributed to the nephelauxetic effect.

The dependence of the F^k parameters on type of compound and the nephelauxetic effect has been studied many times, but always with the aim to better understand the $4f^n$ excited state level energies like in Fig. 4 with respect to the ground state. It was never aimed to describe the VRBE in the ground state. Tanner and Yeung [14] recently collected and analyzed the F^k values for Pr^{3+} in almost 40 different chemical environments. Parameters selected for several representative compounds are compiled in Table IV. That for LaF_3 are roughly 4% and that for La_2O_3 8% smaller than the free ion values.

TABLE IV: F^k parameters for Pr^{3+} in various chemical environments in units of eV. The ones for vacuum are from this work and the others from the compilation in [14].

A	F^2	F^4	F^6	ζ_f	$\beta(3+,A)$	$U(6,A)$
vacuum	8.929	6.495	4.464	0.0948	1	18.05
LaF_3	8.555	6.269	4.068	0.0927	0.958	7.51
$LaCl_3$	8.486	6.228	4.088	0.0927	0.950	6.80
YPO_4	8.410	6.158	4.026	0.0925	0.942	7.09
La_2O_3	8.254	6.141	4.039	0.0913	0.924	6.45

V. DISCUSSION

By combining experimentally determined values for the free lanthanide F^k and $\zeta_{\rm ff}$ parameters with trends that emanate from calculated values, a set of best estimates for the free divalent and free trivalent lanthanides were obtained in Figures 5, 6, 7, 8. With the spin pairing theory one can now compute the contribution $S(q,Q)$ from the Racah E^1, E^3, and $\zeta_{\rm ff}$ parameters to the VRBE $E_{4f}(q,Q,\text{vacuum})$ in the ground states of the lanthanides. The obtained values for $S(q,2+)$ and $S(q,3+)$ are listed in Table V. The values $S(q,3+)$ for the trivalent lanthanides are connected by curve 1) in Fig. 10. The separate contributions from E^1, E^3, and $\zeta_{\rm ff}$ to $S(q,3+)$ are shown as curves 2, 3, and 4.

The most important feature is the hump between q is 7 and 8. Column 7 of Table I shows that E^1 does not contribute for q is 1 to 7 but for Tb^{3+} with q=8 there is a $9E^1(8,3+) \approx 0.57F^2(8,3+) = 6.7$ eV contribution to the e-e repulsion. The contribution slowly decreases to $63E^1(14,3+) - 54E^1(13,4+) = 5.2$ eV for Lu^{3+} as illustrated with curve 2). The spin-orbit contribution illustrated by curve 4) is first slowly increasing with q followed by a 0.71 eV downward jump between q is 7 and 8 and then again slowly increasing. The E^3 contribution creates the oscillating VRBE in the left and in the right hand branch of $S(q,3+)$.

The known $E_{4f}(q,Q,\text{vacuum})$ values in Table II are shown as curves 1) in Fig. 11 and 12. By subtracting the $S(q,Q)$ values one obtains the functions $C(q,Q)$. The values are compiled in Table V and illustrated by curves 2) in Fig. 11 and 12. They are indeed varying smoothly with q. As a test, the $C(q,Q)$ functions were re-calculated by using 5% augmented and 5% reduced values for the free ion F^k parameters. It has only significant effect for $q > 7$

TABLE V: Compilation of the values for $C(q,Q)$ and $S(q,Q)$ as derived from the spin pairing theory and the free divalent and trivalent lanthanide zigzag curves. Energies are in eV, q is the number of electrons in the $4f^q$ ground state of Ln^{2+} and $n = q - 1$ the same for Ln^{3+}.

n	Ln	$C(q,2+)$	$S(q,2+)$	$C(n,3+)$	$S(n,3+)$
0	La	-18.170	-0.116	–	–
1	Ce	-19.723	-0.475	-36.591	-0.167
2	Pr	-21.087	-0.537	-38.370	-0.610
3	Nd	-22.325	0.223	-39.895	-0.705
4	Pm	-23.331	0.962	-41.387	0.187
5	Sm	-24.390	0.789	-42.627	1.072
6	Eu	-25.249	0.329	-43.870	0.900
7	Gd	-25.901	5.566	-44.852	0.402
8	Tb	-26.535	4.625	-45.792	6.422
9	Dy	-27.084	4.194	-46.712	5.487
10	Ho	-27.809	4.969	-47.524	5.089
11	Er	-28.569	5.829	-48.478	5.998
12	Tm	-29.243	5.563	-49.375	6.955
13	Yb	-29.913	4.883	-50.191	6.631
14	Lu	–	–	-51.066	5.816

as illustrated by the two dashed curves above and below curves 2) in Fig. 11 and 12. Note that a discontinuity appears between q is 7 and 8, and unless such discontinuity is supposed to be, we conclude that the used F^k and $\zeta_{\rm ff}$ values must be reliable and that the spin pairing theory is consistent. Curves 3) in Figures 11 and 12 show the VRBE curves after applying the shift and tilt operation of Eq. (11) where for displaying purpose a convenient value of 4 eV for $E(Eu,Q,A)$ was chosen. These curves already mimic quite well the shape of the zigzag curves that are found experimentally for the lanthanides in compounds as in Fig. 1. In this work we intend to add the effect of the nephelauxetic reduction of Racah and ζ parameters on the shape of the binding energy curves. Since F^2 is the most important parameter for the Racah E^1 and E^3 values it is convenient to introduce the nephelauxetic ratio β

$$\beta(Q,A) \equiv \frac{F^2(Q,A)}{F^2(Q,\text{vacuum})} \tag{12}$$

to express not only the reduction in F^2 but also in F^4, F^6, and ζ_{ff}. Furthermore we assume that the reduction is independent on q. The VRBE in the lanthanide ground state in a chemical environment A is now written as

$$E_{4f}(q,Q,A) = C(q,Q) + \beta(Q,A)S(q,Q) + E(Eu,Q,A) + \alpha(Q)(R(Eu,Q) - R(q,Q)) \tag{13}$$

which now contains two compound dependent parameters $\beta(Q,A)$ and the chemical shift for Eu^Q. Note that here the interaction $C(q,Q)$ with the nucleus and [Xe] core is assumed compound independent. If a slight compound dependence were present most likely it will scale with the lanthanide ionic radius and then its effect can be incorporated by a somewhat modified value for $\alpha(Q)$. The chemical shifts for Eu^Q are entirely defined by the $U(6,A)$ parameter via Eq. (9) and (10). Values for $\beta(3+,A)$ for some representative compounds are listed in Table IV and others can be derived from the compilation of Pr^{3+} $F^k(3+,A)$ parameters in[14]. $\beta(3+,A)$ is highest with typical values of 0.96 for the fluoride family of compounds like LaF_3 and lowers progressively when moving to chlorides, bromides, and iodides. Within the oxides it will scale with the electronegativity of the cations that binds the oxygen ligands (P > B > Si > Al). The $U(6.A)$ parameter varies in an opposite fashion which suggests that $\beta(3+,A)$ and $U(6,A)$ are also tightly linked.

The dashed curve 4) in Fig. 12 illustrates the effect of an 8% reduction in $\beta(3+,A)$ on the VRBE for the lanthanide ground states which resembles the situation in La_2O_3 with $U(6,A)$=6.44 eV. The effect for the left hand branch ($q < 8$) of the lanthanide series is barely significant. However, the entire right hand branch ($q > 7$) is lowered by 0.51 eV for Tb^{3+} and 0.46 eV for Lu^{3+}. The same for the divalent lanthanides is demonstrated by the dashed curve 4) in Fig. 11 where the right hand branch is lowered by about 0.4 eV. The VRBE curve for fluorides with $\beta(3+,A) \approx 0.96$ and $U(6,A)$ 7.4 - 7.6 eV will run in between curves 3) and 4). The curves for sulfide and selenide compounds with $U(6,A)$ values down to 6.1 eV are then expected to run below that for La_2O_3.

To explain the nephelauxetic effect, Morrison [17] suggested that a 4f electron will polarize the ligand electrons leading to energy lowering. In fact it describes a correlated motion between the 4f electron and the ligand electrons. The same applies for the 5d electron

of the $4f^{q-1}5d$ configuration. In the case of Ce^{3+} this interaction together with covalence between the 5d-orbital and the ligands was used to establish a relation between the so-called 5d centroid shift and the electronegativity of the cations in the compound in [33]. High electronegative cations bind the anion ligands strongly leading to low polarizability and small nephelauxetic effect. The chemical shift is caused by the screening of the lanthanide charge Q and such screening is also related to ligand polarizability. Indeed an empirical relationship between the $U(6, A)$ parameter of the chemical shift model and the centroid shift for Ce^{3+} was demonstrated in [34]. Considering that ligand polarizability is the common important parameter one may also expect a relationship between $\beta(Q, A)$ and $U(6.A)$.

With $\beta(3+, A)$ ranging from 0.96 for the least polarizable fluoride compounds to about 0.90 for the highly polarizable sulfides and selenides, the lowering of the right hand branch in Fig. 12 is predicted to amount 0.2 eV to 0.6 eV. This gives about 0.4 eV spread over the entire family of inorganic compounds due to the nephelauxetic effect. The changes in the left hand branch are quite insignificant. Electron transfer from a lanthanide to a host band is always accompanied with strong lattice relaxation which leads to typically 0.8 eV wide excitation or absorption bands in optical spectra. With such broad bands the accuracy of level location determination is usually limited to several 0.1 eV, and that is the main reason that a compound dependence of the VRBE curve was never noticed.

The different behavior of Nd from the left hand branch of the VRBE curve from that of Er, Ho, Dy from the right hand branch, as noticed in the TL results of Fig. 2 and the thermobleaching results in Fig. 3, is now explained with a nephelauxetic lowering of the right hand branch of the VRBE curve. This is illustrated in Fig. 13 where the VRBE in the Ln^{2+} ground states from the left hand branch (levels a) and right hand branch (levels c) as used in Fig, 1 are displayed separately. That of Eu^{2+} is placed at zero energy. The Nd^{2+} ground state falls in between that of Er and Ho as observed with TL for oxide compounds like $GdAlO_3$ in Fig. 2. In thermobleaching data for CaF_2, but also for SrF_2 [5] and for BaF_2 [35], Nd appears in between Ho and Dy, a situation that can be obtained by raising the right hand levels c) by 0.15 eV to give the levels b) in Fig. 13. This agrees with the situation shown in Fig. 11 where curve 3) represents the VRBE in a compound without a nephelauxetic reduction or $\beta = 1$. Curve 4) pertains to La_2O_3 with β=0.92, and the right hand branch has lowered by 0.4 eV. Fluorides have typical values of β=0.96 and the right hand levels will raise with about 0.2 eV with respect to that of La_2O_3.

The nephelauxetic lowering also applies to the right hand branch of the $Ln^{3+/4+}$ zigzag curve. It explains why in the sequence phosphates, silicates, aluminates the VRBE in Tb^{3+} from the right hand branch with respect to that in Pr^{3+} from the left hand branch lowers by about 0.1-0.15 eV as concluded from TL-studies in [2]. The cation electronegativity decreases from P, to Si, to Al resulting in decreased oxygen ligand bonding, increased ligand polarizability, and increasing nephelauxetic lowering of the right hand branch.

VI. SUMMARY AND CONCLUSIONS

. We have applied the spin pairing theory of Jørgensen to establish the contribution of 4f interelectron repulsion to the VRBE in the ground state $4f^q\ ^{2S+1}L_J$ multiplets of the free divalent and free trivalent lanthanides. For that we first determined the values of the Slater-Condon F^k and the spin orbit coupling $\zeta_{\rm ff}$ parameters by combining known experimental data with trends from computation. Different from previous work, we have taken the dependence of these parameters on q and on the valence Q (2+, 3+, 4+) of the free lanthanide into account. The derived binding energy of the 4f electrons to the nucleus plus the electrons in the closed [Xe] shells appear to show an expected smooth variation with q. From this we conclude that the used F^k and $\zeta_{\rm ff}$ values are correct and that the spin pairing theory is consistent.

The effect of reduction of the F^k and related E^1 and E^3 Racah parameters due to the nephelauxetic effect on the binding energy when lanthanides are in a chemical environment has been explored. As first order correction the entire right hand branch of the binding energy curve for $q > 7$ is lowered by $9\Delta E^1 \approx 0.566\Delta F^2$ which in practice amounts to several 0.1 eV. This already explains why the VRBE of Nd^{2+} is in between those of Ho and Dy in CaF_2 whereas it is in between those of Er and Ho in oxides. It also explains why the VRBE in the Tb^{3+} ground state lowers by 0.1 to 0.15 eV with respect to that of Pr^{3+} in going from phosphate to silicate to aluminate compounds.

In this work, we ignored a possible compound dependence in the tilt parameter $\alpha(Q)$ and of the smooth function $C(q, Q)$. Such dependence will affect the entire $4f^q$ VRBE curve whereas the nephelauxetic ratio will only affect the right hand branch of that curve. This work has shown that the TL and thermo-bleaching techniques are sensitive enough to compare the VRBE for lanthanides from the left hand branch with that from the right hand

branch with an accuracy of few 0.01 eV. Then with such techniques one may carefully study small changes in the VRBE curve and relate that to a changing nephelauxetic ratio and or tilt factor.

VII. ACKNOWLEDGEMENTS

The author thanks dr. E.R. Radzhabov for sharing his results on thermo-bleaching data presented at the LUMDETR conference in Prague and for bringing reference [5] to his attention.

---

[1] P. Dorenbos, Opt. Materials 69 (2017) 8.

[2] P. Dorenbos, Optical Materials 91 (2019) 333.

[3] P. Dorenbos, Phys. Rev. B 85 (2012) 165107.

[4] Hongde Luo, Adrie J. J. Bos, Pieter Dorenbos, J. Phys. Chem. C 120 (2016) 5916.

[5] V.A. Arkhangelskaya, M.N. Kiseleva, V.M. Shraiber, Soviet Physics Solid State, USSR, 11 (1969) 714 (p.869 in Russian)

[6] C.K. Jørgensen, Mol. Phys. 5 (1962) 271.

[7] C.K. Jørgensen, *Modern Aspects of ligand Field Theory*, North-Holland Publishing Company, Amsterdam, (1971).

[8] D.A. Wensky, W.G. Moulton, J. of Chem. Phys. 53 (1970) 3957.

[9] H.H. Caspers, H.E. Rast, R.A. Buchanan, J. Chem. Phys. 43 (1965) 2124.

[10] W.T. Carnall, P.R. Fields, R. Sarup, The J. of Chem. Phys. 51 (1969) 2587.

[11] O.K. Moune, M.D. Faucher, C.K. Jayasankar, A.M. Lejus, J. Lumin. 85 (1999) 59.

[12] J.S. Griffith, *The theory of Transition-metal Ions* (Cambridge University Press, London, 1961.

[13] C.-G. Ma, M.G. Brik, Q.-X. Li, Y. Tian, Journal of Alloys and Compounds 599 (2014) 93.

[14] Peter A. Tanner, Yau Yuen Yeung, J. Phys. Chem. A 117 (2013) 1072.

[15] E. Antic-Fidancev, M. Lemaitre-Blaise, P. Caro, New J. Chem. 11 (1987) 467.

[16] C. Morrison, D.R. Mason, C. Kikuchi, Phys. Lett. A24 (1967) 607.

[17] C.A. Morrison, J. Chem. Phys. 72 (1980) 1001.

[18] D.J. Newman, J. Phys. chem. solids 34 (1973) 541.

[19] K. Rajnak, B.G. Wybourne, The J. of Chem. Phys. 41 (1964) 565.

[20] I. Kawabe, Geochemical Journal, 26 (1992) 309.

[21] D.A. Johnson, J. Chem. Soc. (a) (1969) 1525.

[22] K.L. Vander Sluis, L.J. Nugent, Phys. Rev. A 6 (1972) 86.

[23] R.D. Shannon, Acta Crystallogr. Sect. A: Cryst. Phys., Diffr., Theor. Gen. Crystallogr. 32 (1976) 751.

[24] Jean-Francois Wyart, Patrick Palmeri, Physica Scripta. 58, (1998) 368.

[25] J.-F. Wyart, W.-U L. Tchang-Brillet, S.S. Churilov, A. N. Ryabtsev, Astronomy and astrophysics 483 (2008) 339.

[26] Jean-Franqois Wyart, Jean Blake, William P. Bidelman, Charles R. Cowley, Physica Scripta, 56 (1997) 446.

[27] Jean-Francois Wyart, Ali Meftah, Jocelyne Sinzelle, Wan-U Lydia Tchang-Brillet, Nissan Spector, Brian R Judd, J. Phys. B: At. Mol. Opt. Phys. 41 (2008) 085001.

[28] A Meftah, S Ait Mammar, J-F Wyart, W-U L Tchang-Brillet, N. Champion, C. Blaess, D Deghiche, O Lamrous, J. Phys. B: At. Mol. Opt. Phys. 49 (2016) 165002.

[29] A. Meftah, J.-F.Wyart, N. Champion, W.-U L. Tchang-Brillet, Eur. Phys. J. D, 445 (2007) 35.

[30] Ali Meftah, Jean-FrancoisWyart, Wan-U Lydia Tchang-Brillet, Christophe Blaess, Norbert Champion, Phys. Scr. 88 (2013) 045305.

[31] P. Dorenbos, J. Lumin. 135 (2013) 93.

[32] Y. Y. Yeung, P. A. Tanner, J. Phys. Chem. A 119 (2015) 6309.

[33] P. Dorenbos, Phys. Rev. B 65 (2002) 235110.

[34] P. Dorenbos, J. Lumin. 136 (2013) 122.

[35] E. A Radzhabov, V. A Kozlovsky,Radiation Measurements 122 (2019) 63.

Figure captions

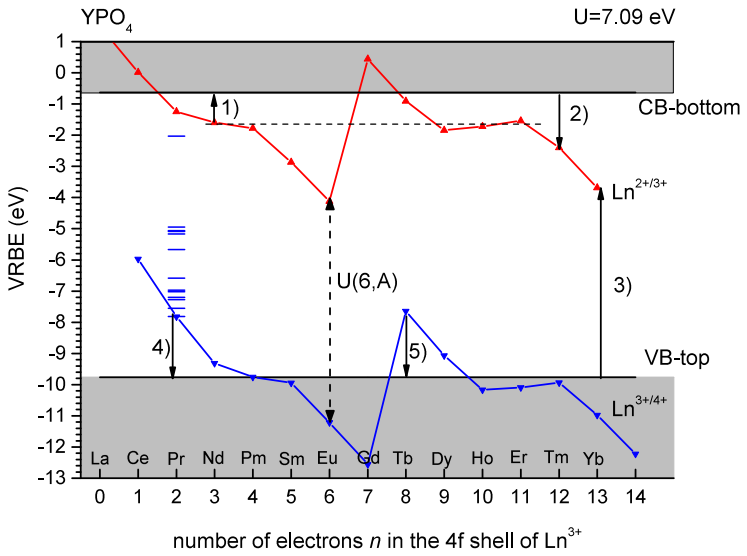

FIG. 1: The vacuum referred binding energy scheme for the divalent and trivalent lanthanide ground state levels in YPO_4. For Pr^{3+} also the VRBE in the excited state $^{2S+1}L_J$ multiplets are drawn. Numbered arrows indicate electron or hole transitions. The horizontal dashed line illustrates that the VRBE for Nd^{2+} is in between that for Ho^{2+} and Er^{2+}.

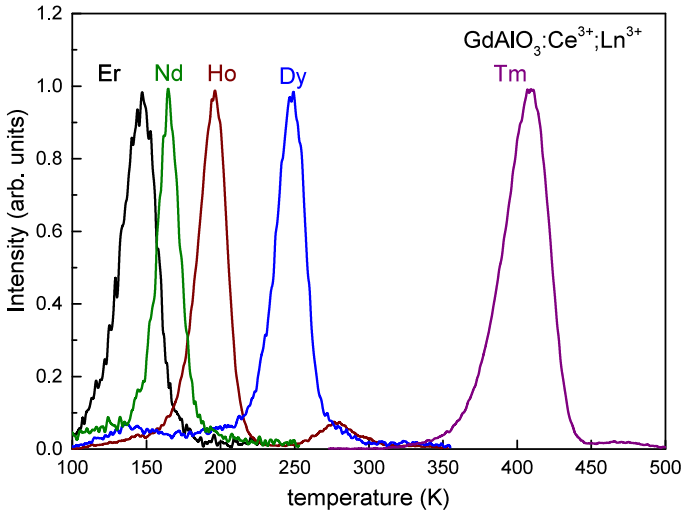

FIG. 2: Thermoluminescence glow curves from $GdAlO_3:Ce^{3+};Ln^{3+}$ (Ln = Er, Nd, Ho, Dy, Tm when monitoring the Ce^{3+} emission at a heating rate of 1K/s. Data are retrieved from [4]

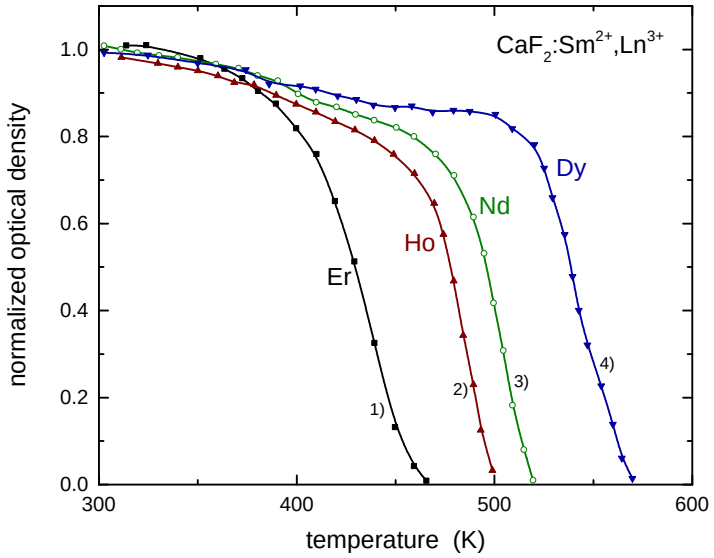

FIG. 3: Thermobleaching curves of 1) Er^{2+}, 2) Ho^{2+}, 3) Nd^{2+}, and 4) Dy^{2+} 4f-5d absorption bands in $CaF_2;Sm^{2+};Ln^{3+}$ (Ln = Er, Ho, Nd, Dy) monitored at a heating rate of 0.25K/s. Data are retrieved from [5].

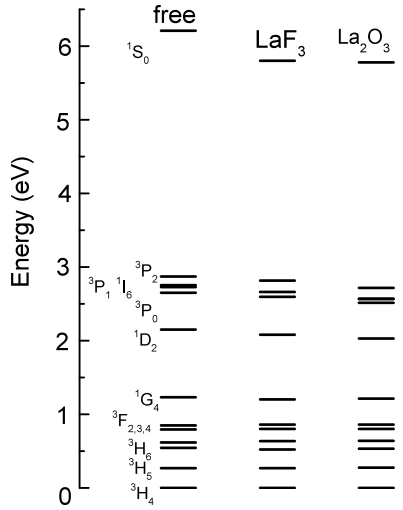

FIG. 4: $4f^2$ energy level energies for Pr^{3+} as free ion in LaF_3 and in La_2O_3. The drawn $^1S_0$ level for La_2O_3 is not from experiment but tentatively placed.

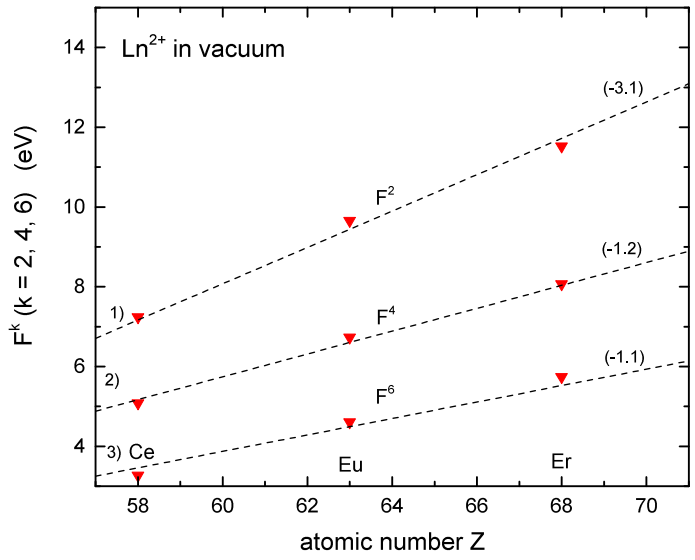

FIG. 5: Experimental data on the F^k parameters for the divalent lanthanides together with the calculated values from [13]. Calculated values were shifted with an amount as indicated in eV within brackets along the dashed lines.

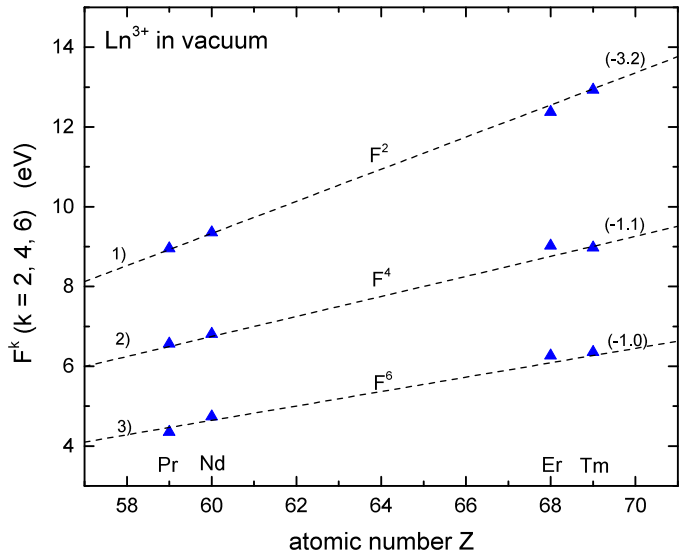

FIG. 6: Experimental data on the F^k parameters for the trivalent lanthanides together with the calculated values from [13]. Calculated values were shifted with an amount as indicated in eV within brackets along the dashed lines.

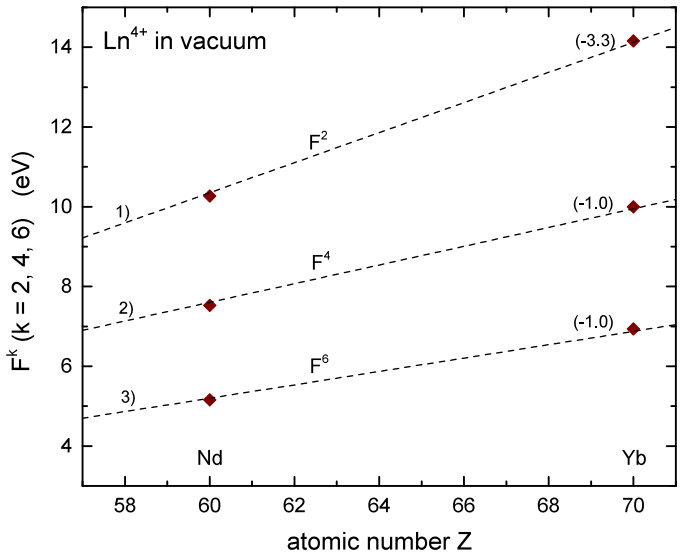

FIG. 7: Experimental data on the F^k parameters for the tetravalent lanthanides together with the calculated values from [13]. Calculated values were shifted with an amount as indicated in eV within brackets along the dashed lines.

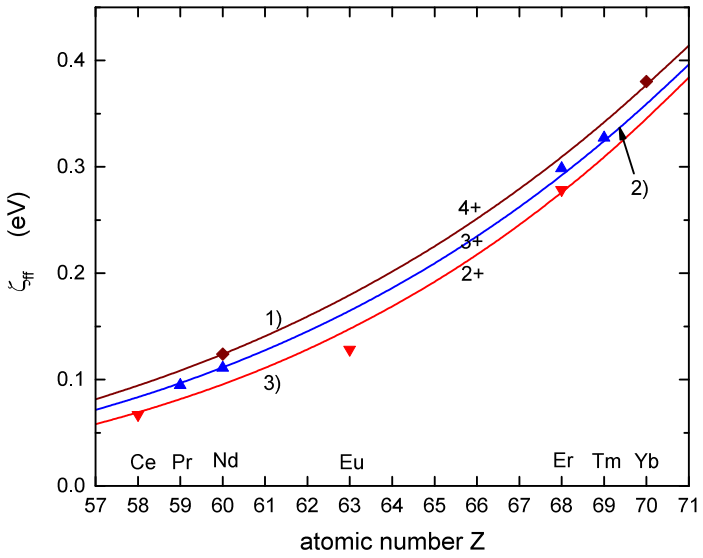

FIG. 8: Experimental data on the ζ_{ff} spin orbit coupling parameter for the free lanthanides together with the calculated values from [13]. Curve 1) calculated values for free Ln^{4+} down shifted by 0.007 eV, 2) for the free Ln^{3+} down shifted by 0.005 eV, 3) for the free Ln^{2+} down shifted by 0.005 eV. The diamond shape, uptriangle, and down triangle data symbols are the experimental values for tetra-, tri-, and divalent lanthanides.

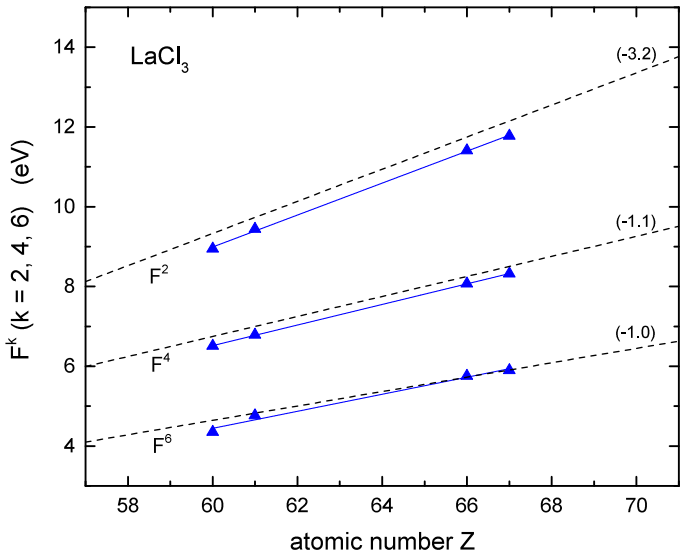

FIG. 9: F^k Slater parameters derived from experimental data for the trivalent lanthanides in $LaCl_3$ from [32]. The dashed lines are based on calculated values for the free lanthanide ions. Calculated values were shifted with an amount as indicated in eV within brackets along the dashed lines to agree best with experimental data.

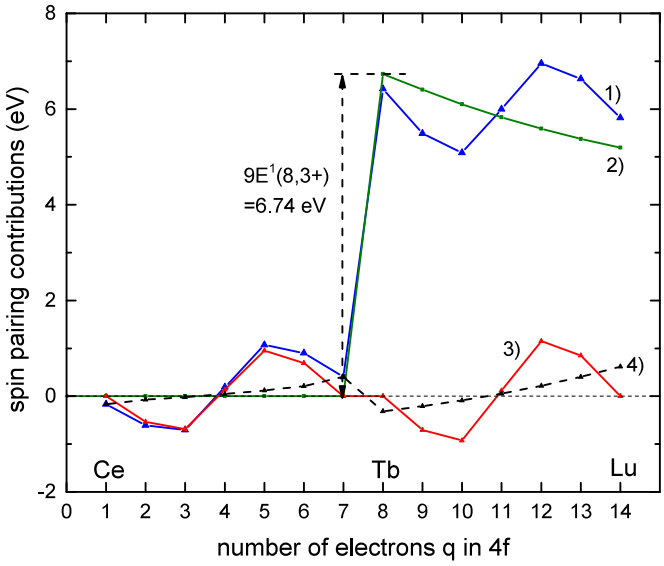

FIG. 10: The contribution of inter 4f-electron Coulomb repulsion $S(q, 3+)$ (curve 1) to the VRBE in the ground state of the free trivalent lanthanides as calculated with the spin pairing theory. 2), 3), and 4) are the separate contributions from E^1, E^3, and $\zeta_{\rm ff}$ to the repulsion.

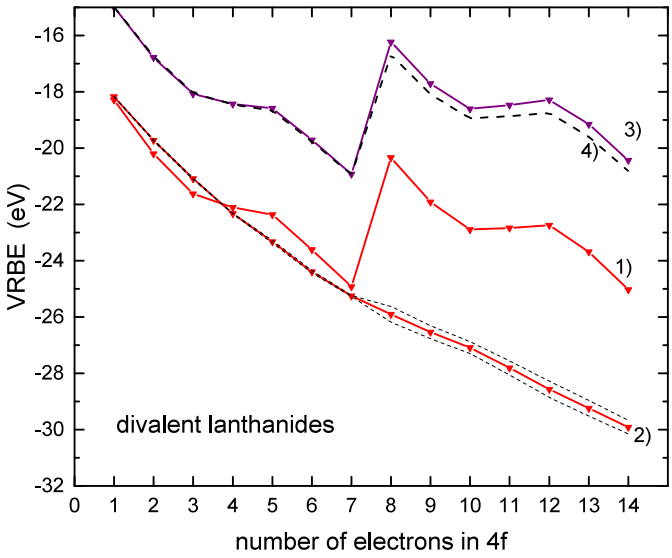

FIG. 11: Curve 1) shows the VRBE $E_{4f}(q, 2+, \text{vacuum})$ in the ground state of the divalent lanthanides. The smooth solid curve 2) is $C(q, 2+)$ obtained by subtracting the calculated spin pairing theory part $S(q, 2+)$ from curve 1). Curves 3) is obtained after applying a chemical shift of 4 eV and a tilt operation with $\alpha(2+)$=0.075 eV/pm. Dashed curve 4) represents the effect of 8% reduced Racah and ζ parameter values on binding energy.

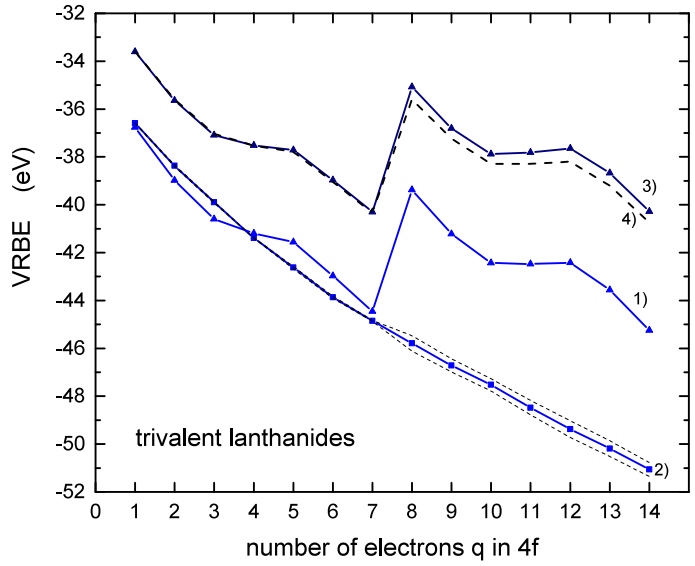

FIG. 12: Curve 1) shows the VRBE $E_{4f}(q, 3+, \text{vacuum})$ in the ground state of the trivalent lanthanides. The smooth curve 2) is $C(q, 3+)$ obtained by subtracting the spin pairing theory part $S(q, 3+)$ from curve 1). Curve 3) is obtained after applying a chemical shift of 4 eV and a tilt operation with $\alpha(3+)$=0.11 eV/pm. Dashed curve 4) represents the effect of 8% reduced Racah and ζ parameter values on binding energy.

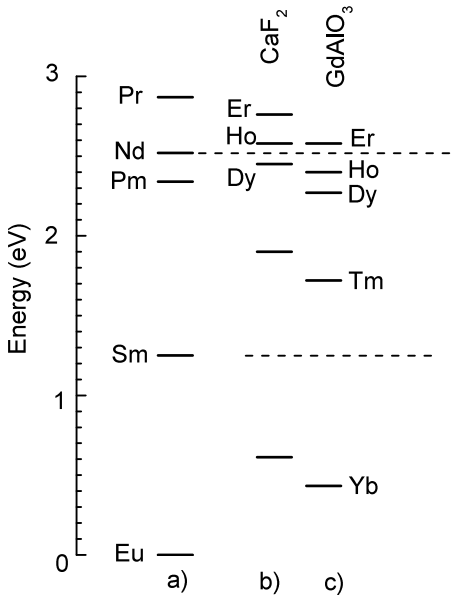

FIG. 13: VRBE energies in the Ln^{2+} ground state with respect to that of Eu^{2+}. Levels a) pertain to lanthanides from the left hand branch of the divalent lanthanide zigzag curve. Levels b) represent the right hand branch lanthanides in fluorides like CaF_2 and levels c) in oxides like $GdAlO_3$.